

Bismuth-doped Ga_2O_3 as candidate for p -type transparent conducting material

Fernando P. Sabino,^{1,*} Xuefen Cai,^{2,†} Su-Huai Wei,^{2,‡} and Anderson Janotti^{1,§}

¹*Department of Materials Science and Engineering,
University of Delaware, Newark, Delaware 19716, USA*

²*Beijing Computational Science Research Center, Beijing 100094, China*

Gallium oxide (Ga_2O_3) is a wide-band-gap semiconductor promising for UV sensors and high power transistor applications, with Baliga's figure of merit that far exceeds those of GaN and SiC, second only to diamond. Engineering its band structure through alloying will broaden its range of applications. Using hybrid density functional calculations we study the effects on adding Bi to Ga_2O_3 . While in III-V semiconductors, such as GaAs and InAs, Bi tend to substitute on the pnictide site, we find that in Ga_2O_3 , Bi prefers to substitute on the Ga site, resulting in dilute $(\text{Ga}_{1-x}\text{Bi}_x)_2\text{O}_3$ alloys with unique electronic structure properties. Adding a few percent of Bi reduces the band gap of Ga_2O_3 by introducing an intermediate valence band that is significantly higher in energy than the valence band of the host material. This intermediate valence band is composed mainly of Bi 6s and O 2p orbitals, and it is sufficiently high in energy to provide opportunity for p -type doping.

Ga_2O_3 is a promising wide-band-gap semiconductor material for power electronics [1–4], solar-blind UV detectors [5, 6], and sensors, with capabilities that go beyond existing technologies due to its very large band gap of about 4.7 eV [5], compared to 3.26 eV in 4H-SiC [7], and 3.44 eV in GaN [8]. The ultra wide gap and large critical electric-field (EC) strength of 8 MV/cm of Ga_2O_3 allow for high temperature and high voltage operation, placing Ga_2O_3 at the top of the most promising semiconductor materials for electronic power switches, just below diamond according to the Baliga's figure of merit (BFOM) due to its high electron mobility and breakdown electric field [3, 9]. Engineering its band structure would open new avenues in device applications.

Ga_2O_3 can be found in five different polymorphs, α [10, 11], β [11, 12], γ [13], δ [11, 14, 15], and ϵ [10, 11, 16], all of which show similar electronic structure: a highly dispersive conduction band derived mostly from Ga 4s orbitals, giving relatively high electron mobility at room temperature, and a flat, low lying valence band derived from O 2p orbitals. These features make Ga_2O_3 easy to be doped n -type, for instance with Si, Ge, and Sn substituting on Ga site, or F substituting on O site [3, 17–19], yet rather difficult (or perhaps impossible) to be doped p -type [20].

Acceptor impurities in Ga_2O_3 induce deep levels in the gap, with rather high ionization energies. For example, predicted acceptor ionization energies of Mg, Cd, Zn or N in β - Ga_2O_3 are higher than 1 eV [21], so that these impurities will not be activated at typical device operating temperatures. Moreover, holes in the valence band of Ga_2O_3 tend to localize on individual O atoms, forming self-trapped holes or small hole polarons [22], giving rise to a broad photoluminescence peak well below the fundamental band gap [23–25].

A possible way to overcome the deep acceptor levels and the self-trapping hole in Ga_2O_3 , thus enabling p -type conductivity, is to raise its valence band. This in principle could be achieved by adding S or Se, whose valence p

orbitals are higher in energy and much more delocalized than the O 2p orbitals. Thus, S or Se substituting on the O sites would lift the valence band of Ga_2O_3 [26, 27], facilitating p -type doping. However, solubility of chalcogenides on the O site is extremely low, in large part due to the very large atomic size mismatch between S or Se and O. Alternatively, one could increase the covalent character of the top of the valence band through a hybridization of O p and metal lone-pair s orbitals [20, 28]. For example, it has been demonstrated that post transition metal additions, for instance, Sn in SnO, Bi in $\text{Ba}_2\text{BiTaO}_6$ or Bi in In_2O_3 [29–32], leads to higher and more delocalized valence bands.

Bi is known to incorporate in the pnictide site in III-V semiconductors as an isovalent group-V anion, such as in InGaAs and InSb [33], or to form compounds with chalcogenides and O, such as Bi_2Se_3 , Bi_2Te_3 [34], and Bi_2O_3 [35, 36], where Bi enters as a trivalent element. Based on atomic size and valence considerations, we explore adding Bi to β - Ga_2O_3 , in the form of dilute $(\text{Ga}_{1-x}\text{Bi}_x)_2\text{O}_3$ alloys. We investigate the site preference, the mixing enthalpy, and the effects of Bi incorporation on the band gap and band-edge positions of the alloys as a function of Bi concentration. We find that Bi prefers to replace Ga at the octahedral sites, and introduces an intermediate valence band, which is significantly higher than the original O 2p band in β - Ga_2O_3 , thus, provides an opportunity for enhanced p -type doping when the defect level and the host occupied level is decoupled. We also show that minimum energy transitions from the new intermediate valence band and the conduction band is still higher than the visible light range, suggesting that Bi doped Ga_2O_3 is a strong candidate for p -type transparent conducting material.

Our electronic structure calculations are based on the density functional theory [37, 38] and the hybrid functional of Heyd-Scuseria-Ernzerhof (HSE) [39, 40] as implemented in Vienna *Ab-initio* Simulation Package (VASP) [41, 42]. The interaction between the va-

lence electrons and the ionic cores are treated using the projected augmented wave potentials [43, 44], with the valence configuration O:2s²2p⁴, Ga:3d¹⁰4s²4p¹, and Bi:5d¹⁰6s²6p³. For structure optimizations, we use the exchange and correlation functional proposed by Perdew-Burke-Ernzerhof and parametrized for solids (PBESol) [45], with a 620 eV cutoff for the plane wave basis set. For the electronic band structure and density of states (DOS) calculations, however, we use the HSE hybrid functional with a 470 eV cutoff.

In the HSE formulation, the exchange functional is separated in long and short range parts [39, 40], and the Hartree-Fock is mixed with the PBE exchange only in the short range part. We used a mixing of 32% Hartree-Fock exchange, which gives a band gap for β -Ga₂O₃ of 4.70 eV, in good agreement with the reported experimental values [5, 46, 47].

For simulating the (Ga_{1-x}Bi_x)₂O₃ alloys we use special quasi random structures (SQS) [48, 49] based on a supercell with 120 atoms. Configurations with Bi concentrations of 2.08%, 4.17%, 6.25%, and 12.5% were generated by replacing 1, 2, 3, and 6 Ga atoms with Bi, respectively. For integrations over the Brillouin zone, we use a 8×8×4 *k*-point mesh for the 10-atom primitive cell of β -Ga₂O₃, and an equivalent *k*-point density for the 120-atom alloy supercells. The optical properties of β -Ga₂O₃ and (Ga_{1-x}Bi_x)₂O₃ alloys are obtained from the calculated frequency-dependent dielectric matrix [50] using the Kramer-Kronig relations with small Lorentzian broadening parameter of 5 × 10⁻⁴ eV. Phonon-assisted indirect transitions or excitonic effects are neglected.

Ga₂O₃ is most stable in the monoclinic β structure belonging to the *C*/2*m* space group, with 10 atoms per primitive cell (2 formula units). There are two inequivalent cation sites, one where each Ga is bonded to four O forming a perfect tetrahedron, and another where Ga is bonded to six O forming a distorted octahedron. Therefore, there are two possibilities for Bi substituting Ga in β -Ga₂O₃. Both configurations were tested, and we find that Bi prefers, by far, to replace the Ga in the octahedral site, with a total energy difference of 0.59 eV per Bi between the two configurations. Note that in α -Bi₂O₃ [51], the Bi atoms are found in high coordinated site, which is similar to the octahedral site in β -Ga₂O₃. Given the large energy difference between the octahedral and tetrahedral configurations, in the following we consider only Bi substituting Ga on the octahedral sites.

The calculated lattice parameters for β -Ga₂O₃, *a*₀ = 3.05 Å, *b*₀ = 12.26 Å, *c*₀ = 5.81 Å, and β = 103.72°, are in good agreement with experimental data, *a*₀^{exp} = 3.04 Å, *b*₀^{exp} = 12.23 Å, *c*₀^{exp} = 5.80 Å, and β ^{exp} = 103.70° [12]. Adding Bi to Ga₂O₃ leads to an increase in the lattice parameters due to the larger Bi atomic radius compared to Ga. The calculated volume per formula unit of Ga₂O₃ and (Ga_{1-x}Bi_x)₂O₃ alloys shows a linear behavior with the concentration *x*, as listed in Table I.

TABLE I. Mixing enthalpy (ΔH^f) per cation, lattice parameter and volume per formula unit for different Bi concentrations (*x*) in (Ga_{1-x}Bi_x)₂O₃ alloys.

System	<i>x</i> (%)	ΔH^f (meV/cation)	Volume (Å ³ /f.u.)
Ga ₂ O ₃	0.00	-	52.68
(Ga _{1-x} Bi _x) ₂ O ₃	2.08	30.40	53.39
(Ga _{1-x} Bi _x) ₂ O ₃	4.17	61.24	54.05
(Ga _{1-x} Bi _x) ₂ O ₃	6.25	88.34	54.75
(Ga _{1-x} Bi _x) ₂ O ₃	12.5	144.16	56.98

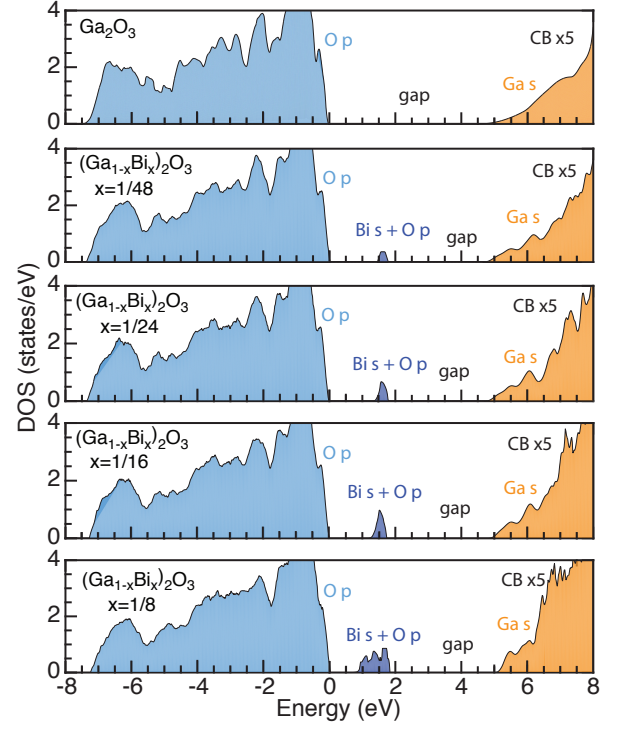


FIG. 1. Calculated density of states (DOS) per formula unit showing the effects of Bi incorporation in β -Ga₂O₃. From top to bottom, Ga₂O₃, and (Ga_{1-x}Bi_x)₂O₃ alloys with *x* = 1/48, *x* = 1/24, *x* = 1/16, and *x* = 1/8. The intermediate valence band derived from a hybridization between Bi 6s and O 2p orbitals are indicated by the dark blue color. The zero in the energy axis is arbitrary placed on top of the O 2p bands, indicated by the light blue color.

The mixing enthalpy of the (Ga_{1-x}Bi_x)₂O₃ alloys are calculated according to the expression:

$$\Delta H^f = E_{tot}[(\text{Ga}_{1-x}\text{Bi}_x)_2\text{O}_3] - (1-x)E_{tot}(\text{Ga}_2\text{O}_3) - xE_{tot}(\text{Bi}_2\text{O}_3), \quad (1)$$

where $E_{tot}[(\text{Ga}_{1-x}\text{Bi}_x)_2\text{O}_3]$ is the total energy of alloy supercell, $E_{tot}(\text{Ga}_2\text{O}_3)$ is the total energy of β -Ga₂O₃, and $E_{tot}(\text{Bi}_2\text{O}_3)$ is the total energy of α -Bi₂O₃. The calculated mixing enthalpy of the alloys are also listed in Table I.

For Bi concentrations lower than 12.5%, the calcu-

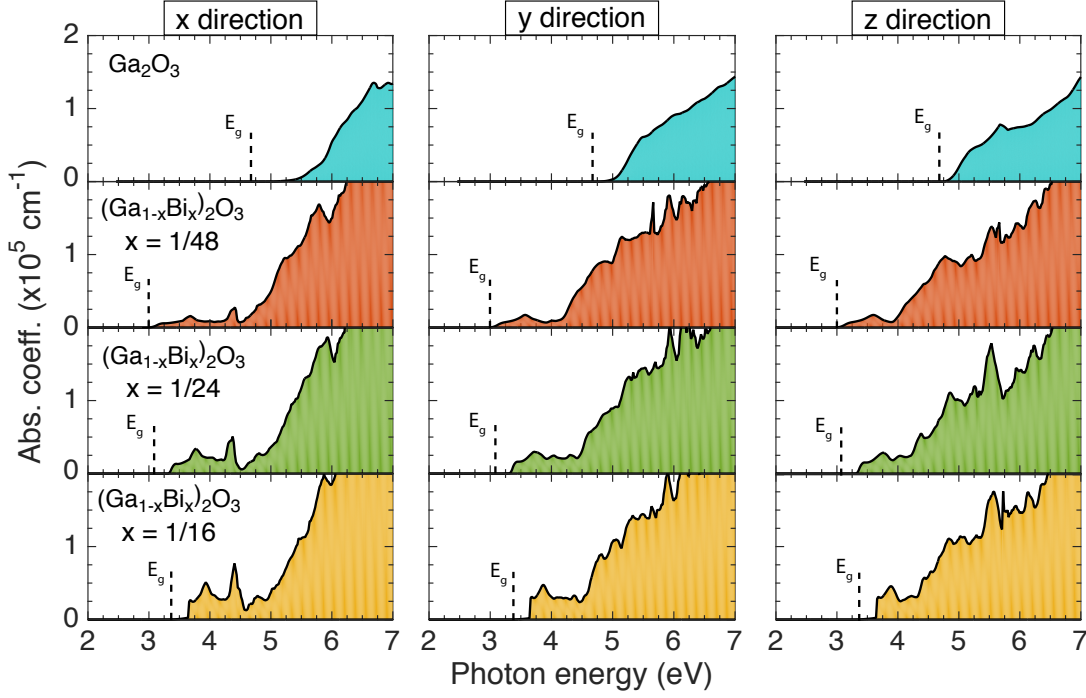


FIG. 4. Absorption coefficients as function of the photon energy for: β -Ga₂O₃, (Ga_{1-x}Bi_x)₂O₃ with $x = 1/48$, $1/24$ and $1/16$. The black vertical dashed line indicate the fundamental.

plied the scissors operator to correct the fundamental band gap according to the HSE results.

First, we observe that Ga₂O₃ shows a sizeable optical anisotropy of the absorption threshold, which is attributed to the anisotropy of the monoclinic crystal structure [54]. Only in the z direction the fundamental and optical band gaps coincide. In the x and y directions, we observe forbidden, or very weak transitions near the fundamental band gap, resulting in optical band gaps that are 0.56 eV and 0.20 eV larger than the fundamental gap.

The incorporation of Bi in Ga₂O₃ in the form of dilute (Ga_{1-x}Bi_x)₂O₃ alloys leads to a sizeable red shift of the absorption threshold due to transitions from the intermediate valence band to the conduction band. The absorption coefficients near the threshold in the alloys is much higher than that in the parent compound Ga₂O₃, and increases with Bi content which we attributed to the increased density of states of the intermediate valence band. We note, however, in the simulations of the random alloys using SQS structures, we find a disparity between the fundamental gap, labeled E_g in Figure 4, and the absorption threshold due to forbidden or weak transitions near the Γ point. This forbidden or weak transitions is explained by the fact that the intermediate valence band and the conduction band have the same symmetry at Γ . In practice, in truly random alloys, we expect the k dependence to disappear due to the lack of long-range symmetry and all bands to fold to the zone center, decreasing the disparity observed in our calculations.

tions.

We now address the possibility of achieving p -type conductivity in the (Ga_{1-x}Bi_x)₂O₃ alloys. Conventional candidate impurities for p -type doping in Ga₂O₃, such as Mg, Cd, Zn and N have been predicted to act as deep acceptors with ionization energies higher than 1 eV [21]. Nevertheless, all the acceptor levels of the candidate impurities for p -type doping are lower than the top of the intermediate valence band in the dilute (Ga_{1-x}Bi_x)₂O₃ alloys. Therefore, if the wavefunctions of the defect levels is decoupled from the host VBM, one may expect that these impurities in the alloy will lead to delocalized holes in the top of the intermediate valence band. However, we note that the interaction between some of the impurities and Bi could lead to coupling effects and ending up in deep acceptor levels. Further studies, therefore is needed to design non-conventional dopants that can lead to shallow defect levels in this system.

In summary, using hybrid density functional calculations we investigate the electronic structure of dilute (Ga_{1-x}Bi_x)₂O₃ alloys. Bi introduces a fully occupied intermediate valence band that is significantly higher in energy than the host original valence band, providing the opportunity to achieve p -type doping in this system, as long as the doped acceptor impurity levels are decoupled from the intermediate states. More importantly, even with the intermediate states, the optical absorption is still beyond the visible range; thus, combined with the p -type doping opportunity, Bi doped Ga₂O₃ is a strong

candidate for p -type transparent material. Therefore, adding Bi to Ga_2O_3 will widen the range of potential applications of this wide-band-gap semiconductor.

FPS and AJ were supported by the National Science Foundation Faculty Early Career Development Program under Grant No. DMR-1652994. XC and SHW were supported by the National Nature Science Foundation of China under Grant No. 11634003 and U1530401. This research was also supported by the the Extreme Science and Engineering Discovery Environment supercomputer facility, National Science Foundation grant number ACI-1053575, and the Information Technologies (IT) resources at the University of Delaware, specifically the high performance computing resources.

* fernandopsabino@yahoo.com.br

† caixuefen@csrc.ac.cn

‡ suhuaiwei@csrc.ac.cn

§ janotti@udel.edu

- [1] M. Higashiwaki, K. Sasaki, A. Kuramata, T. Masui, and S. Yamakoshi, Appl. Phys. Lett. **100**, 013504 (2012).
- [2] M. Higashiwaki, K. Sasaki, T. Kamimura, M. H. Wong, D. Krishnamurthy, A. Kuramata, T. Masui, and S. Yamakoshi, Appl. Phys. Lett. **103**, 123511 (2013).
- [3] M. Higashiwaki, K. Sasaki, H. Murakami, Y. Kumagai, A. Koukitu, A. Kuramata, T. Masui, and S. Yamakoshi, Semicond. Sci. Technol. **31**, 034001 (2016).
- [4] S. J. Pearton, J. Yang, P. H. Cary IV, F. Ren, J. Kim, M. J. Tadjer, and M. A. Mastro, Appl. Phys. Rev. **5**, 011301 (2018).
- [5] M. Orita, H. Ohta, M. Hirano, and H. Hosono, Appl. Phys. Lett. **77**, 4166 (2000).
- [6] R. Suzuki, S. Nakagomi, and Y. Kokubun, Appl. Phys. Lett. **98**, 131114 (2011).
- [7] L. Patrick, W. J. Choyke, and D. R. Hamilton, Phys. Rev. **137**, A1515 (1965).
- [8] O. Madelung, M. Schultz, and H. Weiss, eds., *Semiconductors: Physics of group IV elements and III-V compounds*, Landolt-Börnstein, New Series, Group III, Vol. 17 (Springer-Verlag, Berlin, 1982).
- [9] B. J. Baliga, IEEE Electron Device Letters **10**, 455 (1989).
- [10] S. Yoshioka, H. Hayashi, A. Kuwabara, F. Oba, K. Matsunaga, and I. Tanaka, J. Phys.: Condens. Matter **19**, 346211 (2007).
- [11] F. P. Sabino, L. N. de Oliveira, and J. L. F. Da Silva, Phys. Rev. B **90**, 155206 (2014).
- [12] S. Geller, J. Chem. Phys. **33**, 676 (1960).
- [13] C. O. Areán, A. L. Bellan, M. Mentrui, M. R. Delgado, and G. T. Palomino, Microporous Mesoporous Mater. **40**, 35 (2000).
- [14] R. Roy, V. G. Hill, and E. F. Osborn, J. Am. Chem. Soc. **74**, 719 (1952).
- [15] H. Y. Playford, A. C. Hannon, E. R. Barney, and R. I. Walton, Chem. Eur. J. **19**, 2803 (2013).
- [16] P. Kroll, R. Dronskowski, and M. Martin, J. Mater. Chem. **15**, 3296 (2005).
- [17] M. Orita, H. Hiramatsu, H. Ohta, M. Hirano, and H. Hosono, Thin Solid Films **411**, 134 (2002).
- [18] M. Stefan, von Wenckstern Holger, S. Daniel, S. Florian, and G. Marius, Phys. Status Solidi A **211** (2013).
- [19] J. B. Varley, J. R. Weber, A. Janotti, and C. G. V. de Walle, Appl. Phys. Lett. **97**, 142106 (2010).
- [20] K. H. L. Zhang, K. Xi, M. G. Blamire, and R. G. Egdell, J. Phys.: Condens. Matter **28**, 383002 (2016).
- [21] J. L. Lyons, Semicond. Sci. Technol. **33**, 05LT02 (2018).
- [22] J. B. Varley, A. Janotti, C. Franchini, and C. G. Van de Walle, Phys. Rev. B **85**, 081109 (2012).
- [23] S. Yamaoka and M. Nakayama, Phys. Status Solidi C **13**, 93 (2016).
- [24] Q. D. Ho, T. Frauenheim, and P. Deák, Phys. Rev. B **97**, 115163 (2018).
- [25] S. Yamaoka, Y. Mikuni, and M. Nakayama, J. Phys. Conf. Ser. **1220**, 012030 (2019).
- [26] H. Hiramatsu, K. Ueda, H. Ohta, M. Orita, M. Hirano, and H. Hosono, Thin Solid Films **411**, 125 (2002).
- [27] H. Hiramatsu, K. Ueda, H. Ohta, M. Hirano, M. Kikuchi, H. Yanagi, T. Kamiya, and H. Hosono, Appl. Phys. Lett. **91**, 012104 (2007).
- [28] H. Kawazoe, M. Yasukawa, H. Hyodo, M. Kurita, H. Yanagi, and H. Hosono, Nature **389**, 939 (1997).
- [29] Y. Ogo, H. Hiramatsu, K. Nomura, H. Yanagi, T. Kamiya, M. Kimura, M. Hirano, and H. Hosono, Phys. Status Solidi A **206**, 2187 (2009).
- [30] H. Yabuta, N. Kaji, R. Hayashi, H. Kumomi, K. Nomura, T. Kamiya, M. Hirano, and H. Hosono, Appl. Phys. Lett. **97**, 072111 (2010).
- [31] A. Bhatia, G. Hautier, T. Nilgianskul, A. Miglio, J. Sun, H. J. Kim, K. H. Kim, S. Chen, G.-M. Rignanese, X. Gonze, and J. Suntivich, Chem. Mater. **28**, 30 (2016).
- [32] F. P. Sabino, S.-H. Wei, and A. Janotti, Phys. Rev. Materials **3**, 034605 (2019).
- [33] A. Janotti, S.-H. Wei, and S. B. Zhang, Phys. Rev. B **65**, 115203 (2002).
- [34] P. Shuk, H.-D. Wiemhfer, U. Guth, W. Gpel, and M. Greenblatt, Solid State Ionics **89**, 179 (1996).
- [35] A. Walsh, G. W. Watson, D. J. Payne, R. G. Edgell, J. Guo, P.-A. Glans, T. Learmonth, and K. E. Smith, Phys. Rev. B **73**, 235104 (2006).
- [36] A. Matsumoto, Y. Koyama, and I. Tanaka, Phys. Rev. B **81**, 094117 (2010).
- [37] P. Hohenberg and W. Kohn, Phys. Rev. **136**, B864 (1964).
- [38] W. Kohn and L. J. Sham, Phys. Rev. **140**, A1133 (1965).
- [39] J. Heyd and G. E. Scuseria, J. Chem. Phys. **120**, 7274 (2004).
- [40] J. Heyd, G. E. Scuseria, and M. Ernzerhof, J. Chem. Phys. **124**, 219906 (2006).
- [41] G. Kresse and J. Hafner, Phys. Rev. B **48**, 13115 (1993).
- [42] G. Kresse and J. Furthmüller, Phys. Rev. B **54**, 11169 (1996).
- [43] P. E. Blöchl, Phys. Rev. B **50**, 17953 (1994).
- [44] G. Kresse, Phys. Rev. B **59**, 1758 (1999).
- [45] J. P. Perdew, A. Ruzsinszky, G. I. Csonka, O. A. Vydrov, G. E. Scuseria, L. A. Constantin, X. L. Zhou, and K. Burke, Phys. Rev. Lett. **100**, 136406 (2008).
- [46] H. H. Tappin, Phys. Rev. **140**, A316 (1965).
- [47] N. Ueda, H. Hosono, R. Waseda, and H. Kawazoe, Appl. Phys. Lett. **71**, 933 (1997).
- [48] A. Zunger, S.-H. Wei, L. G. Ferreira, and J. E. Bernard, Phys. Rev. Lett. **65**, 353 (1990).
- [49] S.-H. Wei, L. G. Ferreira, J. E. Bernard, and A. Zunger,

- Phys. Rev. B **42**, 9622 (1990).
- [50] M. Gajdoš, K. Hummer, G. Kresse, J. Furthmüller, and F. Bechstedt, Phys. Rev. B **73**, 045112 (2006).
- [51] G. Malmros, Acta Chem. Scand. **24**, 383 (1970).
- [52] H. Peelaers, D. Steiauf, J. B. Varley, A. Janotti, and C. G. Van de Walle, Phys. Rev. B **92**, 085206 (2015).
- [53] M. Baldini, D. Gogova, K. Irmscher, M. Schmidbauer, G. Wagner, and R. Fornari, Cryst. Res. Technol. **49**, 552 (2014).
- [54] F. P. Sabino, R. Besse, L. N. Oliveira, S.-H. Wei, and J. L. F. Da Silva, Phys. Rev. B **92**, 205308 (2015).